

## Technical Note

### MEASURING LOW CONCENTRATIONS OF FLUORESCENT MAGNETIC NANOPARTICLES BY FLUORESCENCE MICROSCOPY

Zhaolong Shen, Katherine Chen, and Benjamin Shapiro

*Fischell Department of Bioengineering, University of Maryland,  
College Park, Maryland, USA*

*We introduce a method called particle images counting (PIC) to quantify low concentrations of fluorescent magnetic nanoparticles in liquid samples. The sample is diluted with gelatin and a known volume is placed on a microscope slide. The magnetic particles are pulled down to one surface of the slide by a magnet held on the opposing surface before the gelatin is solidified to immobilize the particles. After imaging with fluorescence microscopy, the number of particles is counted using a vision algorithm. Preliminary results are shown to validate this method.*

**Keywords:** fluorescence imaging, fluorescence microscopy, fluorescent nanoparticles, Hough transformation, magnetic nanoparticles, nanoparticles quantification

## 1. INTRODUCTION

Nanoparticles have been widely used as probes and carriers in biological research and clinical practice as fluorescent labels for biological targets (Bruchez et al. 1998) and as contrast agents for magnetic resonance imaging (MRI; Na, Song, and Hyeon 2009). They have also been used for biodetection and separation of pathogens and proteins, separation and purification of biological molecules and cells (Yoshino et al. 2008), and drug and gene delivery for cancer therapy (Salata 2004). However, despite the widespread use of nanoparticles, accurate and low-cost quantitative measurements of nanoparticles in tissue or liquid biological samples remains limited. This is a result of the low availability of precise measuring equipment and the low sensitivity and accuracy of current methods.

Concentrations of nanoparticles can be determined through various methods: by quantifying the elemental composition of the nanoparticles (Thermo Scientific 2012), by measuring signal intensities generated by the nanoparticles (Tziomalos and Perifanis 2010; Krishnan 2010; Ducote, Alivov, and Molloy 2011; Sheth 2003; Nahrendorf et al. 2010; Seevinck et al. 2007; Montet, Ntziachristos, Grimm, and Weissleder 2005; Mortensen, Glazowski, Zavislan, and Delouise 2011; Nasir 2001), or by counting the

Address correspondence to Zhaolong Shen, Fischell Department of Bioengineering, University of Maryland, College Park, MD 20742, USA. E-mail: zhaolong.shen@gmail.com.

## NOMENCLATURE

A	area of coverslip	$I_i$	intensity of $i^{\text{th}}$ identified circle
V	volume of gelatin sample	$\mu$	location parameter of distribution
M	magnification factor of microscope	$\sigma$	scale parameter of distribution
S	area of camera sensor	$\xi$	shape parameter of distribution
IV	sample volume within imaging area		

nanoparticles in a given volume (Christensen, Stenvang, and Godfrey 2004; Roding, Deschout, Braeckmans, and Rudemo 2011).

Here we present particle image counting (PIC) to further increase the availability of nanoparticle quantification methods. Though the PIC method requires nanoparticles suspended in a liquid solution similar to other particle counting methods, it is able to maintain competitive measurement sensitivity and range while requiring relatively simple processes and low-cost measurement equipment.

## 2. MATERIALS AND METHODS

### 2.1. Instrumentation

An inverted fluorescence microscope (IX51, Olympus, Tokyo, Japan) was used for imaging the fluorescent magnetic nanoparticles. Figure 1 shows the schematic of the system, which includes a light source (U-LH100HGAP0, Olympus) with mercury burner, Texas Red filter set (exciter 560/40, dichroic 595, emitter 630/60; Nikon, Tokyo, Japan), microscope objective (UplanFLN 10X, Olympus), and

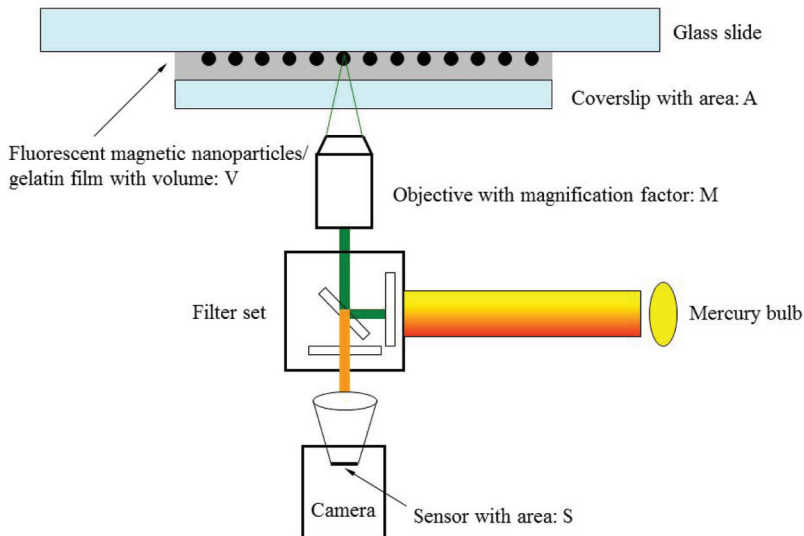


**Figure 1.** The imaging of the fluorescent magnetic nanoparticles/gelatin film in PIC method (color figure available online).

charge-coupled device (CCD) camera (C8484-03G02, Hamamatsu, Japan). The sample was manually positioned using a mechanical stage (IX2-SFR, Olympus).

## 2.2. Sample Preparation

The test nanoparticle solution was prepared by diluting fluorescent magnetic nano-screen MAG/R-D nanoparticles (particle size 200 nm, concentration  $1.3 \times 10^{12}$ /mL) (Chemicell, Berlin, Germany) by 200 times using deionized water. This dilution was then sonicated for 10 minutes. A gelatin/water solution was prepared by adding 2 g of gelatin powder to 100 mL of the deionized water and heating the solution for 2 minutes. A sequence of nanoparticle/gelatin dilutions were prepared from the nanoparticle/water solution by mixing in the gelatin/water solution at different ratios. The final nanoparticle/gelatin dilutions were sonicated for 20 minutes to uniformly distribute the nanoparticles within the gelatin solution. A micropipette was used to place a known volume of the solution droplet on a glass slide. A 12 mm-diameter coverslip was placed on top of the droplet.

The slide was placed into a foam box with ice, inverted so as to position the solution and coverslip on the bottom surface of the slide. To compensate for the limited imaging depth of the microscope, a magnet (N54 neodymium cube magnet, 1.48T,  $0.5 \times 0.5 \times 0.5$  inch<sup>3</sup>, Applied Magnets, Plano, TX, USA) was placed on top of the slide to attract the magnetic nanoparticles to the surface of the glass slide (as shown in Figure 1). The gelatin film solidified with decreasing temperature, this immobilizing the nanoparticles for imaging.

## 2.3. Image Acquisition and Analysis

Once solidified, the nanoparticle/gelatin slide was placed under the fluorescence microscope for imaging. The focus of the microscope was manually adjusted such that the nanoparticles appeared as circles that have minimum overlap with each other. The exposure time of the camera was 0.4 seconds. Three slides were prepared for each nanoparticle concentration, and 10 images were captured at different locations along the film for each prepared slide.

The imaging volume was estimated by determining the imaging area and the thickness of the solution/gelatin film. The thickness of the film can be approximated by dividing the volume of the droplet by the area of the coverslip. The imaging area is the area on the slide corresponding to each image. This area can be well approximated by dividing the area of the CCD sensor by the square of the magnification factor of the microscope. Hence, the imaging volume (IV) can be calculated as

$$IV = V/A \times S/M^2. \quad (1)$$

The particle counting method is illustrated in Figure 2. We employed a well-developed algorithm called the Hough transform (HT) to identify circles in the captured images. First, the raw image was pre-processed using an adaptive histogram equalization function (adapthisteq, Matlab, Mathworks, Natick, MA, USA) to enhance the contrast. The HT algorithm was then used to identify the radii and locations of circles in the enhanced image. To compensate for the nanoparticles

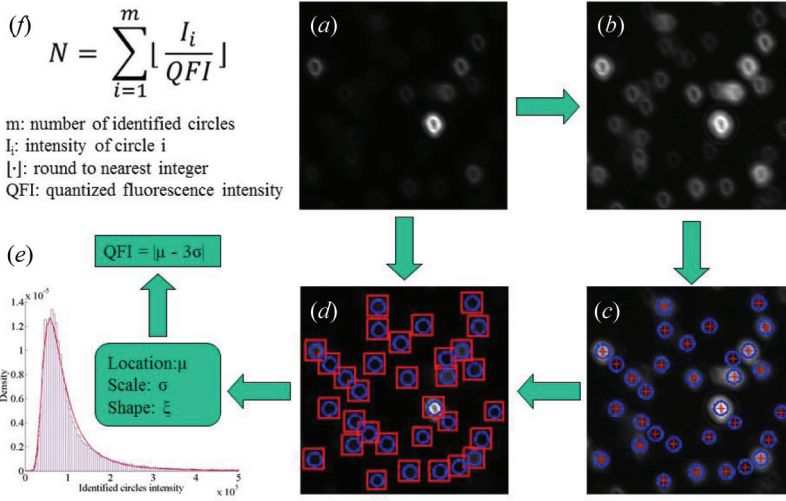


**Figure 2.** Diagram showing estimation of fluorescent nanoparticles number in PIC. (a) Raw image; (b) enhanced image; (c) identified circles; (d) intensities of the identified circles; (e) estimation of quantized fluorescence intensity from the probability distribution of the identified circles intensities; and (f) calculating the total number of the nanoparticles in the image based on the quantized fluorescence intensity value (color figure available online).

agglomeration and to estimate the number of nanoparticles in each identified circles, it is desirable to determine the quantized fluorescence intensity (Q – FI), which corresponds to the intensity of a single fluorescent nanoparticle. In this article, the QFI value is determined from the intensity distribution of the identified circles. For each identified circle, a square window centered on the specific circle was defined in the raw image space. This window size was chosen to include the majority of the pixels showing a fluorescence signal from the particle represented by the circle. The intensity of the circle was then defined as the sum of pixel values inside the window. The probability distribution of the intensities of the identified circles can be well fitted to a generalized extreme value distribution, which can be characterized by three parameters: the location parameter ( $\mu$ ), the scale parameter ( $\sigma$ ), and the shape parameter ( $\xi$ ). Here we define the QFI as

$$QFI = |\mu - 3\sigma|. \quad (2)$$

Thus the number of the nanoparticles can be estimated as

$$N = \sum_{i=1}^m \lfloor I_i / QFI \rfloor, \quad (3)$$

where  $m$  is the number of identified circles in the image,  $\lfloor \cdot \rfloor$  is the floor function, and  $I_i$  is the intensity of circle  $i$ . Finally, the concentration of nanoparticles suspended in solution can be calculated as

$$C = NA/V \times M^2/S. \quad (4)$$

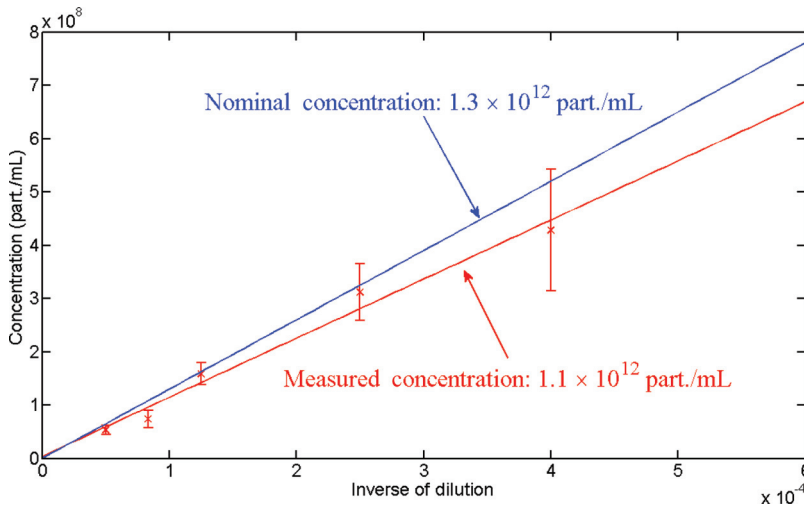


**Figure 3.** The measured concentrations for five different dilutions of a nanoparticle solution (color figure available online).

### 3. RESULTS AND DISCUSSION

The experimental result is shown in Figure 3. The dilution ratios used were 2500, 4000, 8000, 12000, and 20000. The measured values closely align with the nominal values (uncertainty between 12% ~ 26%). By linear fitting to the measured points, the original concentration of the nanoparticles was estimated to be  $1.1 \times 10^{13}$  part./mL, which matched very well with the nominal value  $1.3 \times 10^{13}$  part./mL reported by the manufacturer. The result also indicates that the PIC method yields a more accurate estimate for nanoparticle solutions with low concentration. As the concentration of the nanoparticle solution increases, the distance between the nanoparticles in the image decreases. The performance of the HT algorithm is degraded when the distance between the nanoparticles is decreased to a point where fluorescence interference occurs. The PIC method can also be used to find the agglomeration distribution of the nanoparticles in the solution. After the QFI value is determined, the number of nanoparticles in each identified circle in the image can be calculated. By calculating the number of nanoparticles in all identified circles, the probability distribution of the nanoparticles number in each agglomeration can be determined statistically.

### 4. CONCLUSION AND FUTURE WORK

In this article, we have presented a low-cost scheme for measuring low concentrations of fluorescent magnetic nanoparticles suspended in solution using a fluorescence microscope. We have validated the measuring capability and accuracy of this scheme through experiment. Our results indicate that this methodology allows one to measure nanoparticles suspended in a solution with concentrations ranging from  $10^6 \sim 10^8$ /mL. This method can also be used to quantify the agglomeration of the nanoparticles. However, the primary limitation of this scheme is the determination

of QFI. In this article, the QFI was defined arbitrarily in Equation (2) through trial and error. The future work of this research will focus on the mathematical modeling and error analysis of this method to find an optimal QFI function for samples with given backgrounds, contaminations, and agglomerations.

## REFERENCES

- Bruchez, M., M. Moronne, P. Gin, S. Weiss, and A. Alivisatos. 1998. Semi-conductor nanocrystals as fluorescent biological labels. *Science* 281 (5385): 2013–2016.
- Christensen, P., J. Stenvang, and W. Godfrey. 2004. A flow cytometric method for rapid determination of sperm concentration and viability in mammalian and avian semen. *Journal of Andrology* 25 (2): 255–264.
- Ducote, J., Y. Alivov, and S. Molloy. 2011. Imaging of nanoparticles with dual-energy computed tomography. *Physics in Medicine and Biology* 56 (7).
- Krishnan, K. M. 2010. Biomedical nanomagnetism: A spin through possibilities in imaging, diagnostics and therapy. *IEEE Transactions on Magnetics* 46 (7): 2523–2558.
- Montet, X., V. Ntziachristos, J. Grimm, and R. Weissleder. 2005. Tomographic fluorescence mapping of tumor targets. *Cancer Research* 65 (14): 6330–6336.
- Mortensen, L. J., C. Glazowski, J. Zavislan, and L. Delouise. 2011. Near-IR fluorescence and reflectance confocal microscopy for imaging of quantum dots in mammalian skin. *Biomedical Optics Express* 2 (6): 1610–1625.
- Na, H. B., I. Song, and T. Hyeon. 2009. Inorganic nanoparticles for MRI contrast agents. *Advanced Materials* 21 (21): 2133–2148.
- Nahrendorf, M., E. Kelihir, B. Marinelli, P. Waterman, P. Feruglio, L. Fexon, M. Pivovarov, et al. 2010. Hybrid PET-optical imaging using targeted probes. *Proceedings of the National Academy of Sciences* 107 (17): 7910–7915.
- Nasir, H. 2001. Fluorometric method for the simultaneous quantitation of differently-sized nanoparticles in rodent tissue. *International Journal of Pharmaceutics* 214 (1–2): 55–61.
- Roding, M., H. Deschout, K. Braeckmans, and M. Rudemo. 2011. Measuring absolute number concentrations of nanoparticles using single-particle tracking. *Physical Review E* 84 (3): 031920.
- Salata, O. 2004. Applications of nanoparticles in biology and medicine. *Journal of Nanobiotechnology* 2 (1): 3.
- Seevinck, P. R., J. Seppenwoolde, T. Wit, J. Nijssen, F. Beekman, A. Schip, and C. Bakker. 2007. Factors affecting the sensitivity and detection limits of MRI, CT, and SPECT for multi-modal diagnostic and therapeutic agents. *Anti-Cancer Agents in Medicinal Chemistry* 7 (3): 317–334.
- Sheth, S. 2003. Squid biosusceptometry in the measurement of hepatic iron. *Pediatric Radiology* 33 (6): 373–377.
- Thermo Scientific. 2012. An elementary overview of elemental analysis. Thermo Scientific. <http://www.thermo.com/eThermo/CMA/PDFs/Articles/articlesFile18407.pdf> (accessed 2012).
- Tziomalos, K. and V. Perifanis. 2010. Liver iron content determination by magnetic resonance imaging. *World Journal of Gastroenterology* 16 (13): 1587–97.
- Yoshino, T., H. Hirabe, M. Takahashi, M. Kuhara, H. Takeyama, and T. Matsunaga. 2008. Magnetic cell separation using nano-sized bacterial magnetic particles with reconstructed magnetosome membrane. *Biotechnology and Bioengineering* 101 (3): 470–477.